Core/shell structural transformation and brittle-to-ductile transition in nanowires

Zaoshi Yuan, Ken-ichi Nomura, and Aiichiro Nakano
Collaboratory for Advanced Computing and Simulations, Department of Physics and Astronomy, Department of Computer Science, Department of Chemical Engineering and Materials Science, University of Southern California, Los Angeles, California 90089-0242, USA

(Received 11 January 2012; accepted 25 March 2012; published online 11 April 2012)

Nanowires (NWs) exhibit thermo-mechanical properties that are distinct from their bulk properties, and their understanding is critical for the reliability, manufacturability, and optimization of a wide range of devices consisting of NWs. Here, molecular-dynamics simulation reveals a rich size-temperature "phase diagram" for the mechanical response of a zinc-oxide NW under tension. For smaller diameters and higher temperatures, transitions are found from brittle cleavage to structural transformation-mediated brittle cleavage to ductile failure. Atomistic mechanisms of the unique nano-thermo-mechanical behavior are elucidated as a consequence of surface-structural relaxation, which in particular predicts spontaneous formation of a core/shell structure under tension. The nano-thermo-mechanical phase diagram resolves controversies between previous experiments and theory, and the predicted "intrinsic" core/shell structure may find device applications. © *2012 American Institute of Physics*. [http://dx.doi.org/10.1063/1.3703303]

Recent advances in nanomechanical experiments are revealing unique mechanical properties of nanowires (NWs) and nanopillars, which are distinct from their bulk counterparts.[1–3] A notable example is recent discovery of ductility in nanopillars made of nominally brittle materials below a critical diameter.[4–7] Understanding such nano-thermo-mechanical properties[8] is critical for the reliability, manufacturability, and optimization of a wide range of devices consisting of NWs. A prototypical example is zinc oxide (ZnO), for which various unique nanomechanical properties have been reported.[9,10] For example, both experimental and theoretical studies have shown the stiffening of NW for smaller diameters.[11–13] Molecular-dynamics (MD) simulation has shown that [0001]-oriented ZnO NWs transform from wurtzite (WZ) to body-centered-tetragonal (BCT) structure under uniaxial tension,[14] which leads to unique fracture behavior.[15] Structural transformation to graphitic structure has also been predicted theoretically below a critical diameter.[16] However, none of these structural transformations has been observed experimentally,[15] and this controversy demonstrates the lack of our understanding of the mechanical properties of ZnO NWs.

A major unsolved problem is the size and temperature dependence of the failure behavior of ZnO NWs. For example, brittle cleavage has been observed experimentally,[15] while a MD simulation shows super-ductility.[17] A complete size-temperature "phase diagram" for the mechanical response of a ZnO NW under tension would be a valuable tool for understanding nanomechanical experiments and for better reliability and manufacturability of devices utilizing NWs. Here, MD simulation of [0001]-oriented ZnO NW under tension provides such a nano-thermo-mechanical phase diagram, which reveals transitions from brittle cleavage to structural transformation-mediated brittle cleavage to ductile failure for smaller diameters and higher temperatures. The phase diagram also explains why theoretically proposed structural transformations have not been observed in experiments,[15] and resolves the brittle vs. ductile controversy between experiments[15] and theory.[17] Furthermore, atomistic mechanisms of the unique nano-thermo-mechanical behavior are elucidated as a consequence of "incipient" surface-structural relaxation, which exists even in the absence of tension, and in particular predicts spontaneous formation of "intrinsic" core/shell structures under tension, as opposed to extrinsic core/shell structures[18] constituted of different atomic species.

We perform MD simulation of a [0001]-oriented ZnO NW with six $\{01\bar{1}0\}$ sidewalls (Fig. 1(a)). The NW diameter is $D = 2.5$, 5, and 10 nm, with an aspect ratio $L/D = 8$ (L is the NW length).[19] The atomic positions are first relaxed by the steepest-descent method to obtain a local minimum-energy configuration, where period boundary condition is applied along the NW axis. Subsequently, NWs are slowly heated up to a target temperature and thermalized for 10 ps. In total, 11 samples are prepared for each diameter at temperatures ranging from 100 to 1400 K. Detailed information on the MD simulation is provided in supplementary material.[20] In particular, the interatomic potential[21] used in the MD simulation reproduces the contraction of Zn-O bonds near the $(01\bar{1}0)$ surface of WZ crystal up to a depth of six atomic layers, which is in agreement with *ab initio* calculation results[22] (see Fig. S1 in Ref. 20).

The surface relaxation of the $\{01\bar{1}0\}$ sidewalls mentioned above leads to unique structural features of the NWs. To show these features, Figs. 1(b) and 1(c) visualize the change of surface bonds. Figure 1(b) is the top view of slip-vector field of the smallest NW (2.5 nm in diameter). As described in supplementary material, the slip vector quantifies the displacement of atoms relative to their neighbors in the reference system (i.e., a system without defect), and contains information about the slip plane and Burgers vector.[23] Figure 1(c) shows the bond-network structure of the same

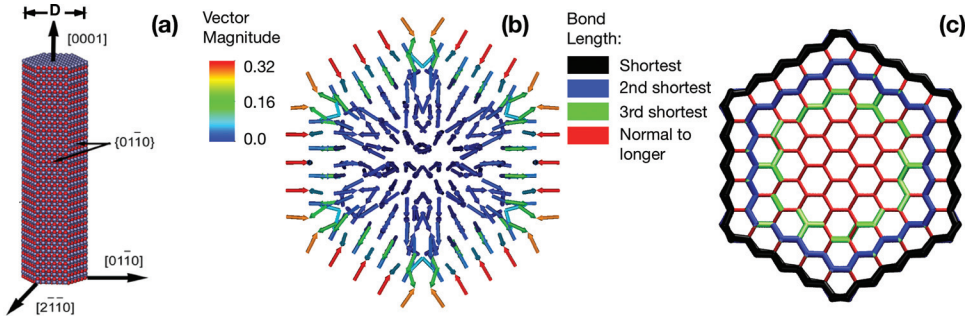

FIG. 1. (a) Schematic of simulated ZnO NW with diameter D. (b) and (c) show the incipient core-shell structure of ZnO NW with $D = 2.5$ nm at temperature 5 K. (b) Top view of color-coded slip-vector field. (c) Top view of bond network, where the bonds are colored in black (shortest bond), blue (2nd shortest), and green (3rd shortest). Normal or elongated bonds are colored in red.

NW, where different levels of bond contraction are color-coded. The outermost layer of the NW has the shortest bond length, which is colored black. The third-layer atoms have the 2nd shortest bond length (colored blue). The 3rd shortest bond length is colored green, and normal-length or elongated bonds are in red. From the slip-vector field and the bond-network structure, we can see that the first layer of atoms moves towards the inner core of the NW as a result of the bond contraction. At the same time, the atomic bonds in the next layer, which moves outward with less magnitude, are stretched. Similar behavior is exhibited for the subsequent atomic bilayers, i.e., the 3rd to 4th layers and the 5th to 6th layers, with less magnitude. This "incipient" core/shell structure, with a six-layer-thick shell of different symmetry from the core, will play a major role in the mechanical response of the NWs as shown below.

After thermalization, uniaxial tensile tests are performed along the [0001] direction, in which the NWs are elongated by 0.1% at every 15 ps until they break. (As shown in Ref. 5, Young's modulus and other mechanical properties are rather insensitive to the strain rate, except for the fracture strength.) Stress-strain curves of ZnO NWs of different diameters at temperature 100 K in Fig. S2 (Ref. 20) exhibit the size effect on fracture strength[24] (i.e., the stress at which the NW fractures). The fracture strength increases from 8.5 to 15 GPa as the diameter of the NW decreases from 10 to 2.5 nm. The strength of the NW thus decreases by 43% as the diameter increases by four-fold. The slope of the stress-strain curve also changes systematically with the diameter. Young's modulus $E_{\langle 0001\rangle}$ is obtained by linear fitting of the stress-strain curve in the strain range of 0%–1%.[25] The calculated $E_{\langle 0001\rangle}$ is a decreasing function of the diameter: 129, 120, and 113 GPa for $D = 2.5$, 5, and 10 nm, respectively. The calculated stiffening of NWs with decreasing diameter is in accord with previous theoretical and experimental observations, and can be explained by the larger ratio of the volume of the bond-contracted (and thus stiffer) outer shell to that of the normally bonded inner core (see Fig. 1(c)).[11–13]

We next study the effect of temperature on the stress-strain curve. The stress-strain curves of the smallest NW of diameter 2.5 nm at different temperatures between 100 and 1400 K are shown in Fig. 2(a). Fracture strength decreases as the temperature is increased. Also, Young's modulus decreases by 12% (from 129 to 114 GPa) from temperature 100 to 500 K. The NW fails by cracking at strains of ~9% and 7% at 100 and 500 K, respectively. At 600 K, the stress-strain curve exhibits a distinct feature, i.e., it is divided into 2 stages. The first stage is below strain ~9%, and the second stage is between strain 9% and 12%. Similar two-stage stress-strain curves were observed in previous MD simulations.[14,15] In spite of this unique behavior, however, the NW still fails by cleavage at 600 K, and the stress drops to 0 sharply at the failure strain. Above 1200 K, on the other hand, the stress gradually decreases at large strains but does not become 0, indicating the onset of ductility. Similar behavior is observed for NWs of diameter 5 and 10 nm. As shown in Figs. 2(b) and 2(c), the onset of the two-stage behavior is 1000 and 1200 K for $D = 5$ and 10 nm,

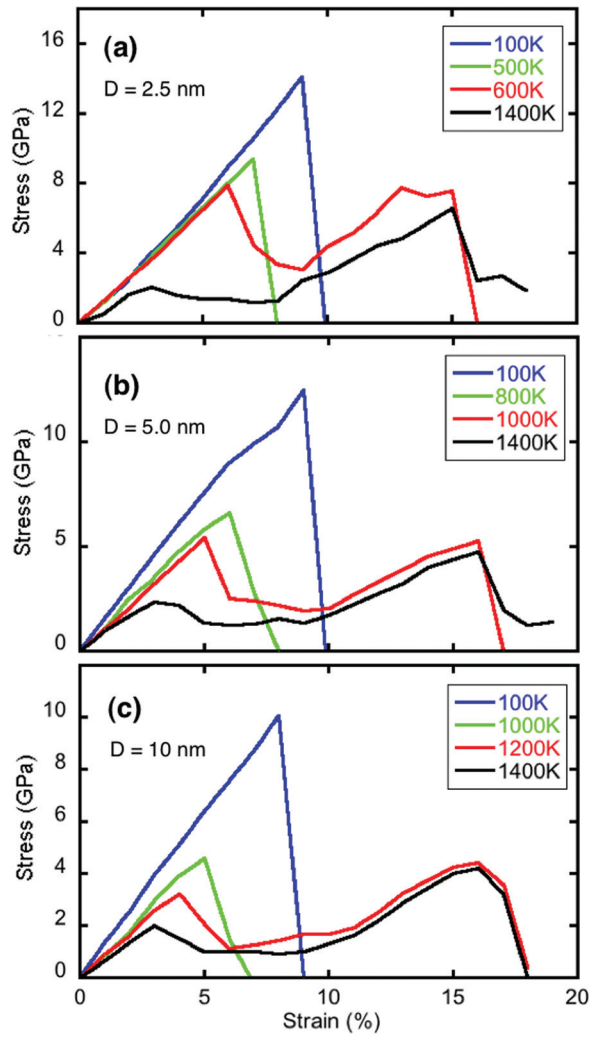

FIG. 2. Temperature dependence of the tensile stress-strain curve of ZnO NW with diameter $D = 2.5$ nm (a), 5 nm (b), and 10 nm (c).

respectively. The onset of ductility for $D = 5$ nm is 1400 K, whereas the 10 nm NW still fails in a brittle manner even at the highest simulated temperature of 1400 K. It should be noted that at room temperature no simulated NW exhibits the two-stage stress-strain curve, in accord with existing experimental studies, thus resolving the previous controversies between experiments and theory mentioned before.[15,17] Especially, ZnO NW exhibits both brittle and ductile behaviors, as well as the two-stage stress-strain relation, depending on the size and temperature. The mechanical response of ZnO NW is a sensitive function of the size and temperature, and comparison between experiment and theory must be made carefully at equivalent conditions.

In order to understand the atomistic mechanisms underlying the two-stage stress-strain curves in Fig. 2, we analyze the atomic configurations of the NW before and after the transition to the two-stage stress-strain behavior. Figure 3 shows slip-vector fields and atomic structures during the ascending part of the second stage in the stress-strain curve for diameter 5 nm at temperature 1000 K. Fig. 3(a) is the top view of the slip-vector field, and Fig. 3(b) is the side view of a 1.5 nm slab marked by black dashed lines in Fig. 3(a). Figure 3(a) shows that atoms in the outermost layer (with the shortest bonds) move radially on the (0001) plane, while the second-layer atoms move axially along the [0001] direction with a larger magnitude. Similar behavior is observed for the 3 rd and 4th layers as well as for the 5th and 6th layers. These six surface layers correspond to those in the incipient shell in the initially relaxed NW (Figs. 1(b) and 1(c)). In the inner core of the NW, in contrast, the radial movements of the odd-numbered layers are disordered, while the vertical movements of the even-numbered layers are still pronounced. The corresponding atomic bond structures are shown in Figs. 3(c) and 3(d), which respectively show the top and side views. In Fig. 3(c), the shell loses the hexagonal (HX) symmetry of the original WZ crystal. In Fig. 3(d), the shell atoms form alternating 8 - and 4-atom rings, instead of the 6-atom rings in WZ, which is a consequence of the alternating layer-by-layer bond-length contraction and elongation under tension explained above. This structural transformation in the NW shell under tension is identical to the WZ-to-BCT transformation reported in previous simulations.[14,15] As for the inner core structure, it still retains the original HX symmetry in the (0001) plane and the $[01\bar{1}0]$ direction. With its characteristic atomic movements (every even layer moves axially), the core forms a graphite-like structure reported in a tensile test along the [0110] direction.[16] Our simulation thus predicts spontaneous formation of a core/shell structure under tension. This structural transformation is accompanied by a large stress relaxation, resulting in the two-stage stress-strain response. Similar NW failure mediated by structural transformation has been reported for $SiSe_2$.[26] It should be pointed out that the "intrinsic" core/shell structure here (as opposed to extrinsic core/structures constituted of heterogeneous atomic species[18]) originates directly from the incipient core/shell structure in the unstretched NW shown in Fig. 1.

It is worth mentioning that the surface-structural relaxation induced mechanical response is most pronounced in thin NWs. For example, the volume ratio of the shell to the inner core is 8/1 for $D = 2.5$ nm, and is 1/2 for $D = 10$ nm. The ratio becomes smaller for larger diameters, where the intrinsic core/shell effect is less significant. In addition to the temperature effect explained above, this size dependence may partially explain existing controversies between experiment and theory.[15] Furthermore, the origin of the core/shell mechanism suggests that it should be sensitive to surface functionalization.

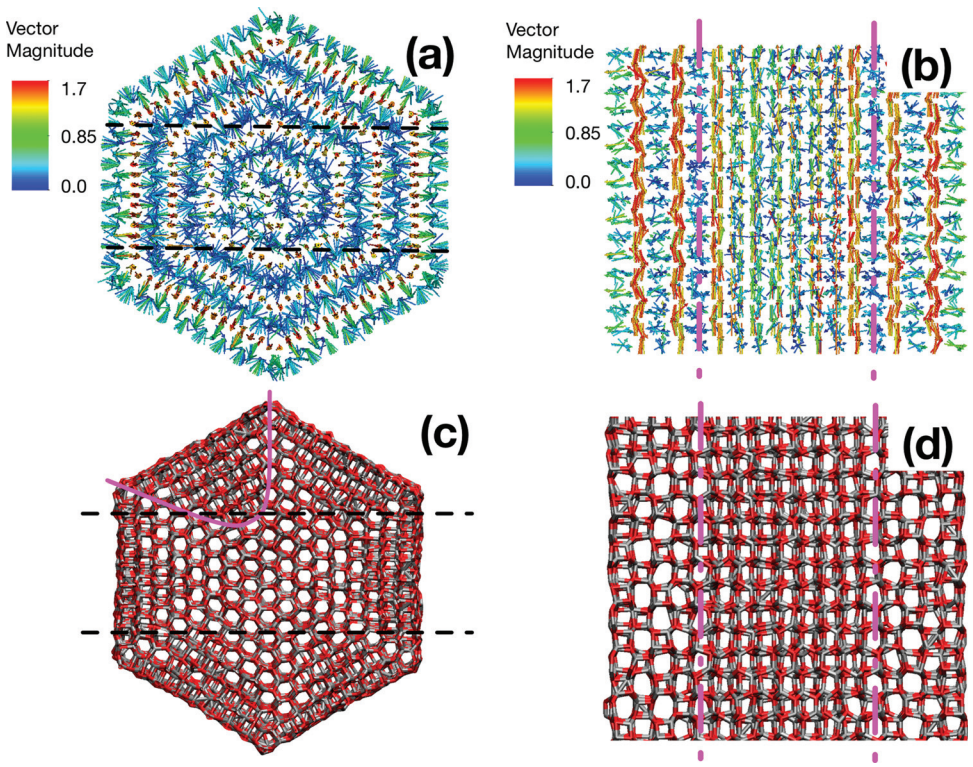

FIG. 3. Intrinsic core-shell structure of the NW under tension for diameter 5 nm at temperature 1000 K. (a) Top view of slip-vector field. (b) Side view of slip-vector field of the slab shown in dashed black lines in (a). (c) Atomic structure of the same NW as shown in (a). Magenta dashed line delineates BCT- and HX-transformed zones. (d) Atomic structure of the same NW slab as in (b). Magenta dashed lines delineate the BCT and HX zones.

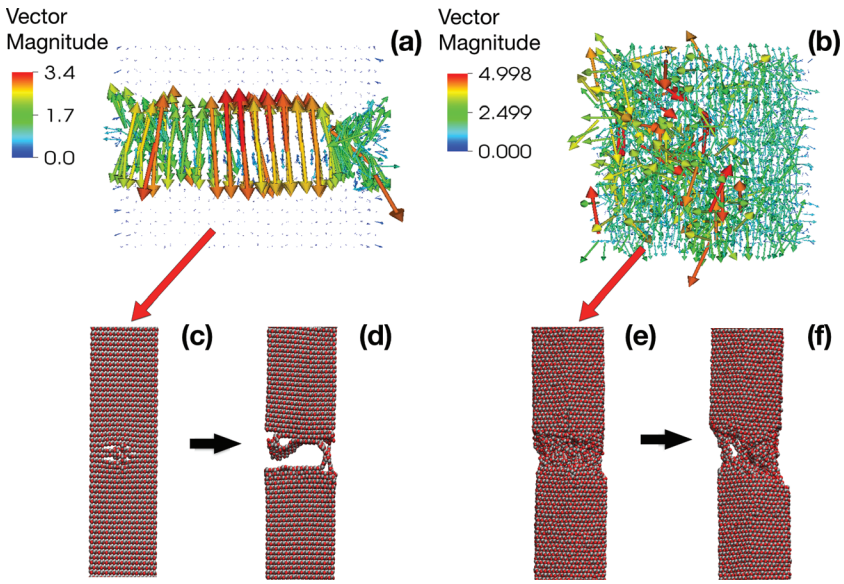

FIG. 4. Snapshot of slip-vector field of the 5 nm NW right before failure at temperature 100 K (a) and 1000 K (b). Corresponding atomic positions before (c) and after (d) failure at 100 K, and those before (e) and after (f) failure at 1000 K. Slip-vector field in a 1.5 nm-thick slab at the center of the NW is shown.

In order to understand the second transition at a higher temperature, we again use the slip-vector analysis, which can distinguish whether the NW fails by cleavage fracture or ductile failure (i.e., whether the initial event responsible for the failure is the nucleation of a crack or a dislocation).[5] If the vector displacement relative to the reference system with no defect (same direction as Burgers' vector) is parallel to the slip plane, it corresponds to a dislocation. On the other hand, vector displacement predominantly perpendicular to a plane signifies mode-I crack opening.

Figure 4(a) shows a side view of slip-vector field in the 5 nm NW at temperature 100 K, for which the stress-strain curve exhibits brittle behavior. The vectors in the central core are mostly perpendicular to the (0001) crack plane, indicating mode-I fracture. The snapshots of atomic positions before and after failure in Figs. 4(c) and 4(d) indeed confirm the brittle cleavage. It should be noted that the crack initiates in the inner core of the NW and then propagates to the stiffer bond-contracted shell. A similar core/shell model has been proposed for explaining the size-dependent Young's modulus,[11–13] and our simulation results show that the core/shell structure essentially dictates the failure mode of the NW. The slip-vector field in Fig. 4(b) shows that the NW fails in a ductile manner at 1000 K, where the vectors deviating from the [0001] direction indicate mixed-mode fracture. The corresponding snapshots of atomic positions in Figs. 4(e) and 4(f) show necking, which is a signature of ductile failure.

The above analysis confirms the existence of brittle-to-ductile transition (BDT),[4,5] in addition to the surface-mediated structural transformation under tension as described before. For example, the structural transformation occurs at 600 K, followed by BDT at 1000 K, in the smallest NW ($D = 2.5$ nm). Figure 5 summarizes the size-dependence of the two transformation temperatures. This size-temperature phase diagram can be used to understand nanomechanical experiments on ZnO NWs.

In summary, MD simulation reveals rich size-temperature dependence for the mechanical response of ZnO NW under tension, resulting from the intrinsic core/shell structure, which in turn originates from the incipient core/shell structural motifs due to surface relaxation of unstretched NW. The resulting size-temperature phase diagram shows transitions from brittle cleavage to structural transformation-mediated brittle cleavage to ductile failure for smaller diameters and higher temperatures. This nano-thermo-mechanical phase diagram resolves several controversies between previous nanomechanical experiments and theory, and is expected to help design and understand nanomechanical experiments. Furthermore, the predicted intrinsic core/shell structure may find device applications due to different mechanical (and possibly electronic) properties of the

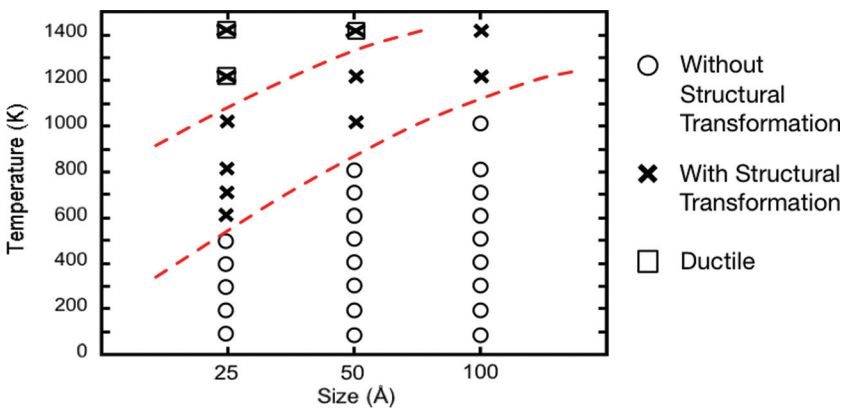

FIG. 5. Size-temperature phase diagram for the mechanical response of [0001]-oriented ZnO NW, where the temperature is scaled by the melting temperature.[27] The circles and crosses denote response without and with structural transformation, respectively. The squares denote ductile failure, otherwise, the fracture is brittle.

BCT shell and HX core, along with their atomically sharp interface.

This work was partially supported by DOE—BES (simulation of size-temperature phase diagram)/EFRC (core/shell structural analysis). Simulations were performed at the University of Southern California using the 20925-processor Linux cluster at the High Performance Computing Facility.

[1]J. R. Greer and J. T. M. De Hosson, Prog. Mater. Sci. **56**(6), 654–724 (2011).
[2]T. Zhu and J. Li, Prog. Mater. Sci. **55**(7), 710–757 (2010).
[3]Y. B. Wang, H. J. Joyce, Q. A. Gao, X. Z. Liao, H. H. Tan, J. Zou, S. P. Ringer, Z. W. Shan, and C. Jagadish, Nano Lett. **11**(4), 1546–1549 (2011).
[4]F. Ostlund, K. Rzepiejewska-Malyska, K. Leifer, L. M. Hale, Y. Y. Tang, R. Ballarini, W. W. Gerberich, and J. Michler, Adv. Funct. Mater. **19**(15), 2439–2444 (2009).
[5]K. W. Kang and W. Cai, Int. J. Plast. **26**(9), 1387–1401 (2010).
[6]H. Guo, P. F. Yan, Y. B. Wang, J. Tan, Z. F. Zhang, M. L. Sui, and E. Ma, Nature Mater. **6**(10), 735–739 (2007).
[7]D. C. Jang and J. R. Greer, Nature Mater. **9**(3), 215–219 (2010).
[8]S. Keten, Z. P. Xu, B. Ihle, and M. J. Buehler, Nature Mater. **9**(4), 359–367 (2010).
[9]Z. L. Wang, J. Phys.: Condens. Matter **16**(25), R829–R858 (2004).
[10]J. Elias, C. Levy-Clement, M. Bechelany, J. Michler, G. Y. Wang, Z. Wang, and L. Philippe, Adv. Mater. **22**(14), 1607–1612 (2010).
[11]C. Q. Chen, Y. Shi, Y. S. Zhang, J. Zhu, and Y. J. Yan, Phys. Rev. Lett. **96**(7), 075505 (2006).
[12]R. Agrawal, B. Peng, E. E. Gdoutos, and H. D. Espinosa, Nano Lett. **8**(11), 3668–3674 (2008).
[13]X. J. Liu, J. W. Li, Z. F. Zhou, L. W. Yang, Z. S. Ma, G. F. Xie, Y. Pan, and C. Q. Sun, Appl. Phys. Lett. **94**(13), 131902 (2009).
[14]J. Wang, A. J. Kulkarni, F. J. Ke, Y. L. Bai, and M. Zhou, Comput. Methods Appl. Mech. Eng. **197**(41–42), 3182–3189 (2008).
[15]R. Agrawal, B. Peng, and H. D. Espinosa, Nano Lett. **9**(12), 4177–4183 (2009).
[16]L. X. Zhang and H. C. Huang, Appl. Phys. Lett. **90**(2), 023115 (2007).
[17]L. Dai, W. C. D. Cheong, C. H. Sow, C. T. Lim, and V. B. C. Tan, Langmuir **26**(2), 1165–1171 (2010).
[18]L. J. Lauhon, M. S. Gudiksen, C. L. Wang, and C. M. Lieber, Nature (London) **420**(6911), 57–61 (2002).
[19]A smaller aspect ratio of $L/D = 4$ did not provide converged thermomechanical properties, which may be attributed to the absence of long-range phonons in the axial direction.
[20]See supplementary material at http://dx.doi.org/10.1063/1.3703303 for simulation details.
[21]P. Vashishta, R. K. Kalia, A. Nakano, and J. P. Rino, "Interaction potential for zinc oxide: molecular dynamics studies of thermal and mechanical properties of crystalline and amorphous ZnO" (unpublished).
[22]B. Meyer and D. Marx, Phys. Rev. B **67**(3), 035403 (2003).
[23]J. A. Zimmerman, C. L. Kelchner, P. A. Klein, J. C. Hamilton, and S. M. Foiles, Phys. Rev. Lett. **87**(16), 165507 (2001).
[24]S. Hoffmann, F. Ostlund, J. Michler, H. J. Fan, M. Zacharias, S. H. Christiansen, and C. Ballif, Nanotechnology **18**(20), 205503 (2007).
[25]Stress is calculated using the Virial formula [see, e.g., M. Parrinello and A. Rahman, J. Appl. Phys. **52**(12), 7182–7190 (1981)], reflecting the volume change due to elongation and Poisson effect. Accordingly, the calculated stress is the true value.
[26]W. Li, R. K. Kalia, and P. Vashishta, Phys. Rev. Lett. **77**(11), 2241–2244 (1996).
[27]The calculated melting temperture, 2050 K, agrees well with the experimental value, 2248 K